Preparation of Fe Substituted ZnO Nanoparticles and Investigation of Their Magnetic Behaviors

Hasanpour, Ahmad*+

Physics Department, Ahvaz Branch, Faculty of Science Islamic Azad University, Ahvaz, I.R. IRAN

ABSTRACT: *Nano-powders of diluted magnetic semiconductor $Zn_{1-x}Fe_xO$ ($0.0 \leq x \leq 0.1$) were prepared via the sol-gel auto-combustion method. Crystal structure and phase identification carried out by X-Ray Diffraction (XRD) analysis. Mean crystallite size of the powders was estimated by Scherrer's formula. As M-H loops of the Fe substituted ZnO showed ferromagnetic behavior. The results of X-Ray Photoelectron Spectroscopy (XPS) showed that there is a mixture of Fe^{3+} and Fe^{2+} ions in all Fe substituted samples. Antiferromagnetic interaction between neighboring Fe^{3+}-Fe^{2+} ions suppressed the ferromagnetic behavior of the samples at higher doping concentrations of Fe.*

KEYWORDS *Diluted magnetic semiconductor; Zinc oxide; Sol-gel auto-combustion method.*

INTRODUCTION

Diluted Magnetic Semiconductors (DMS) are a class of oxides such as TiO_2 and ZnO which are substituted with a small number of magnetic ions. DMSs have been studied intensively due to possible ferromagnetic behavior at room temperature and ability to control spin and charge of carriers simultaneously [1]. These materials are used extensively in spintronic devices. [2]

Among II-VI host semiconductors, Fe substituted ZnO is a multifunctional material and has applications in the optoelectronic [4,5], spintronics [2], biosensors [6] and ultraviolet lasing devices[7]. Ferromagnetism has been observed in many types of transition metal substituted oxide semiconductor nanostructures, but the mechanism of the observed ferromagnetism in these oxides is still not clear. In some literature the point defects, oxygen, and Zn vacancies and interstitials have been considered to be responsible for ferromagnetism [8-12]. For synthesizing ZnO nanoparticles various methods such as hydrothermal [13], sol-gel [14] and co-precipitation [15] have been used.

In this work, Fe substituted ZnO nanoparticles have been prepared via the sol-gel auto-combustion method and their magnetic properties have been investigated. We demonstrate that the observed ferromagnetic property in Fe substituted zinc oxide is an intrinsic behavior and is independent of iron clusters or secondary phases [16].

EXPERIMENTAL SECTION

Sample preparation

Substituted-ZnO nanoparticles were prepared by sol-gel auto-combustion method. Zinc nitrate (Zn $(NO_3)_2$, $6H_2O$), Iron (III) nitrate (Fe$(NO_6)_3$,$6H_2O$) and citric acid $C_6H_8O_7$ all of the analytical grade were used as raw materials. The raw materials were stoichiometrically weighed and dissolved in 100cc deionized water. The solution was heated at $80 \pm 5°C$ and stirred
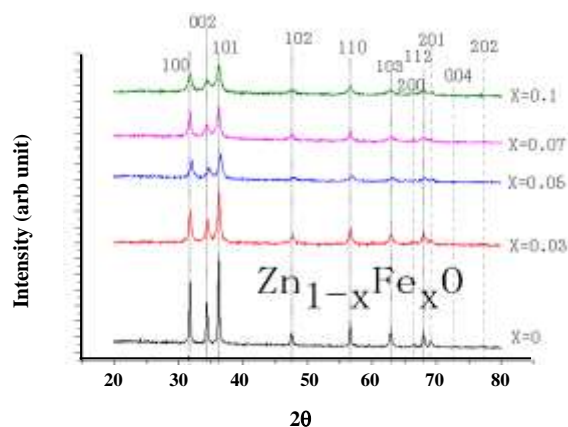
Fig. 1: X-ray diffraction patterns of Zn₁₋ₓFeₓO for different x values.

Fig. 2: Expansion of (101)peak for different Fe concentration that shows the shift of the main peak.

at this temperature until a brown gel was achieved. The gel was then dried in an oven at 240 °C. Combustion took place at this temperature and the sample changed into ashes after a very short time. Nitrate to citrate ratio is a key point to obtain an effective ignition. In this work, a ratio of 2 was obtained by trial and error. The burned black powders were then annealed at 500°C for 5 hr. and their colors changed to white for x=0 and then to yellow and light brown with increasing impurities.

RESULTS AND DISCUSSION
X-Ray Diffraction(XRD) analysis

The XRD patterns of all sintered samples with different x values have been shown in Fig 1. As can be seen, all samples are in the hexagonal wurtzite structure with space group (P63mc) and can be well indexed to the hexagonal phase ZnO (JCPDS card no. 36-1451) without any extra phases. Also, X-ray patterns (Fig.2) showed that by increasing Fe content, (101) peak is shifted to higher Bragg angles. This increase can be attributed to different values of ionic radius of Fe that substituted for Zn^{2+} in ZnO lattice, which leads to the change of lattice parameters. The zigzag nature of this variation may be due to the substitution of Fe ion in the forms of Fe^{2+} and Fe^{3+} (with bigger and smaller ionic radiuses than the radius of Zn^{2+} respectively) for Zn^{2+} in the crystal lattice. This phenomenon shows a good agreement with the following results of XPS. Presence of the part of Fe^{2+} in the form of Fe^{3+} showed that there are some cation (Zn^{2+}) vacancies in the ZnO structure as reported earlier [17]. and this deformation is due to the electrical charge compensation.
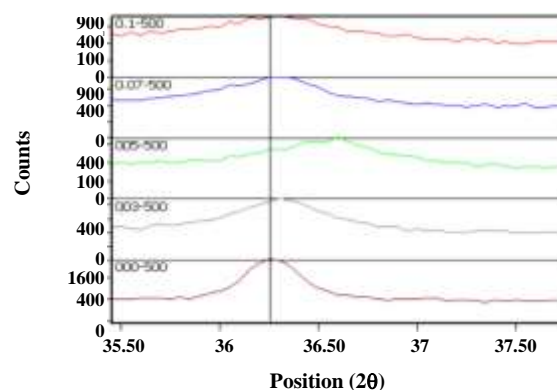
The crystallite sizes of pure ZnO and Fe: ZnO were estimated by Scherrer's formula, using full width at half maximum (FWHM) of the XRD main peaks that they were in the range of 34to 24.28 nm for ZnO and a different value of Fe in Fe-ZnO respectively. As can be seen in Fig. 1, the intensity of diffraction peaks decreases as a function of Fe concentration .that was corresponded to the determination of crystallite sizes by Scherer's formula, this phenomena showed that the crystallinity of the ZnO had decreased due to Fe-doping. Similar observation has been reported by other studies [16].

SEM analysis

The mean particle sizes of the samples were measured by SEM micrographs (Fig.3) that were in the range of 60 to 40 nm for pure ZnO and Fe-ZnO with different Fe concentration respectively. As is observed in this figure, with increasing x values, the mean particle size of the samples are decreased but the agglomeration of the samples is increased.

FT-IR analysis

The FT-IR spectra of pure and Fe substituted ZnO samples have been shown in Fig.4 As can be seen, all the peaks are in the range of 400 to 600 cm^{-1} which belong to the Zn-O band oscillations. In this region, the peak that appears at 445cm^{-1} in pure ZnO, belongs to Zn-O band and is ascribed to the E1(TO) vibration mode. However, the position of this peak in the case of 3 and 5% Fe substituted samples tend to the 435 and 425 cm^{-1} respectively .this peak for 7% substitution of tending to right
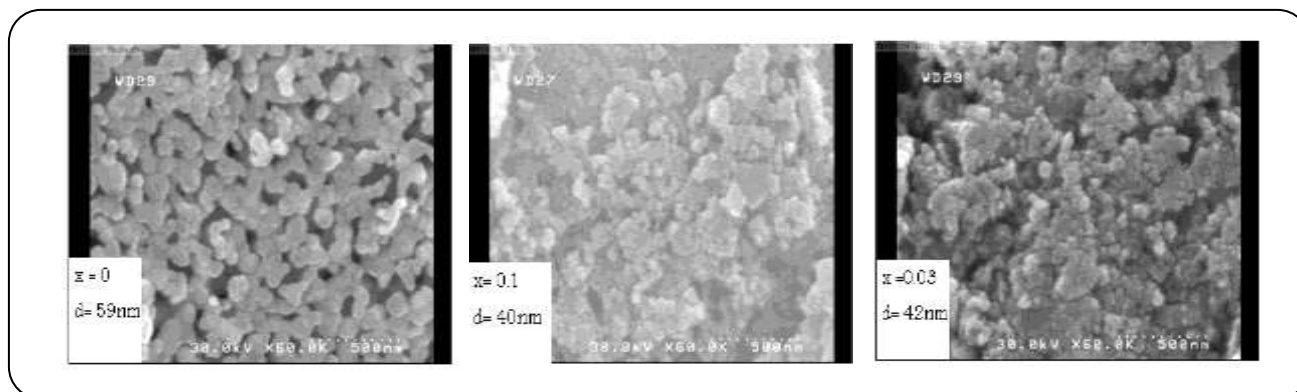
Fig.3: SEM micrographs of $Zn_{1-x}Fe_xO$ with different x values, as marked on the micrographs.
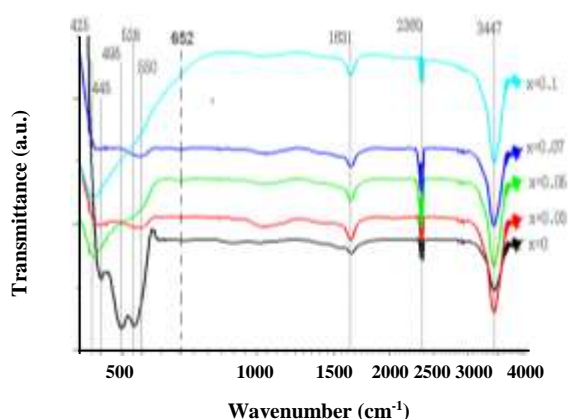

Fig. 4: FT-IR spectra of single phase $Zn_{1-x}Fe_xO$ nano-powders for different x values.

hand 435and again for 10%came to 425 cm^{-1}. This red and blue shift reflects that Zn-O-Zn network variation is a zigzag shape with respect to x value. This shows that the Fe substitution in different samples is a mixture of Fe^{+2} and Fe^{+3} with different ratios of Fe^{2+}/Fe^{3+}.The peaks that appear at495 and 528 cm^{-1} are related to surficial phonons [18,19], while the peak at 652 cm^{-1}, found only in the Fe-doped samples are characteristic of a Fe–O stretch [20,21]. The surface phonon modes normally appear when the prepared particles are smaller than the size of the IR wavelength. The peaks at 1631 and 3447cm^{-1} are related to H-O-H and O-H band states are associated with moisture absorbed from the environment by the samples. Finally the peak at 2360 cm^{-1} may be related to C=O band oscillations.

XPS Spectroscopy

For more information about the different ionization states of Fe in ZnO lattice, X-ray photoelectron spectroscopy (XPS) was used. Fig.5 shows the XPS spectra of $Zn_{1-x}Fe_xO$ for (x=0.05 and 0.07) .The diagrams show the peaks related to Zn, Fe, O and C elements in the samples. The position of each peak was calibrated by C.As shown in this figure, the peaks at1021 and 1044 eV in both samples are related to Zn 2p$^{3/2}$ and Zn 2P$^{1/2}$. These peaks confirm the existence of Zn in the form of Zn^{2+} on the surface of the samples. According to this figure, the presence of Fe ions on the lattice is in the form of 2P$^{3/2}$ and 2P$^{1/2}$ and with energy bands of and 723eV respectively. But the peaks for Fe^{2+} are located at 710.3 and 722.3eV and for Fe^{3+} at 710 and 724 eV [16].Hence the valence state of Fe is believed to be a mixture of Fe^{2+} and Fe^{3+}.

Magnetic measurements:

Fig. 6 shows the room temperature M-H curves of Fe substituted samples. It is obvious that pure ZnO shows diamagnetic behavior at room temperature whereas Fe substituted samples show ferromagnetism at room temperature. The interesting point is that by increasing Fe content, the magnetization of the samples with x=0.03 and 0.05 are increased. However, the curve related to the sample with x=0.07 shows a lower magnetization than that of the sample with x=0.05. In addition, the curves keep going up with an increasing magnetic field. This seems that the ferromagnetic property observed in substituted zinc oxides is an intrinsic behavior which is independent of existing iron clusters or secondary phases [16]. This phenomenon can be discussed by intrinsic magnetic theory (RKKY) [22,23]. This theory suggests that the origin of ferromagnetism at room temperature for Fe- substituted zinc oxide can be related to the interring
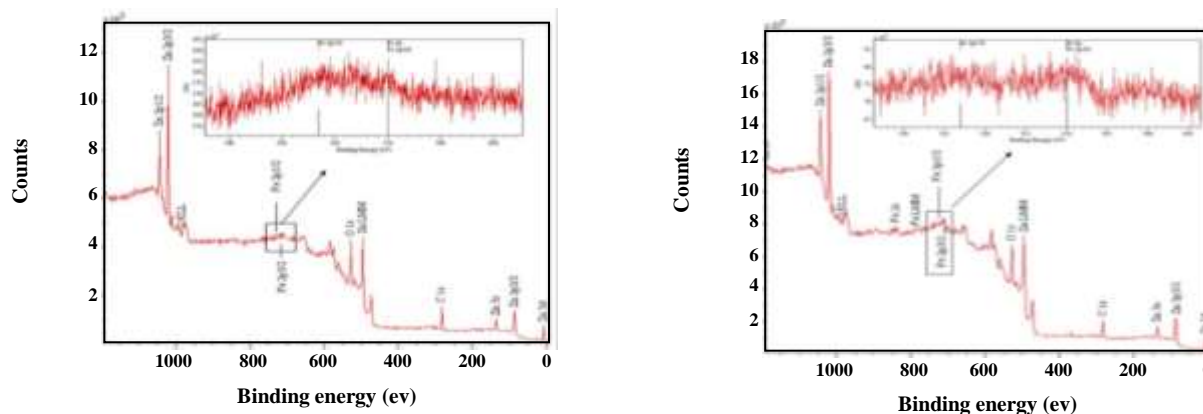
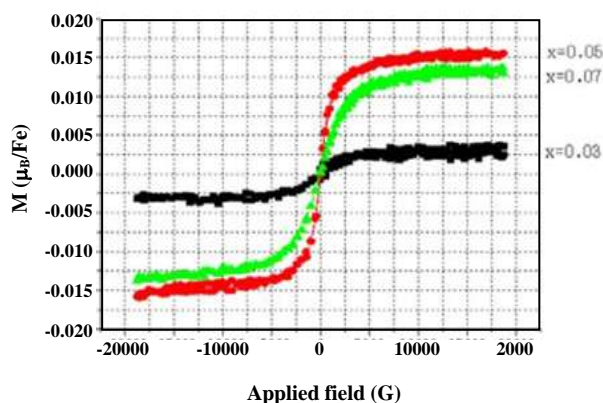*Fig. 5: XPS spectra of $Zn_{1-x}Fe_xO$ for (a) x=0.05% and (b) x=0.07%.*

Fig. 6: Room temperature M-H curves of $Zn_{1-x}Fe_xO$ for x=0.03, 0.05 and 0.07.

of Fe^{2+} and Fe^{+3} ions into the exchange interaction between the conduction electrons and the electrons of Fe^{+3} and Fe^{2+} ions can be an important factor in any ferromagnetic order [24]. The important point in Fig.6 is that the observed magnetic effect is related to the interaction between Fe^{3+} and Fe^{2+} ions and in this case the magnetic effect due to ferromagnetic order of these ions is negligible. The d sub-shell electron configuration for Fe^{2+} is $3d^6$ and for Fe^{3+} is $3d^5$. So if any of these ions (and not interaction between them) is the cause of ferromagnetic order, the magnetic moment per Fe ion must be $4\mu_B$ and $5\mu_B$ for Fe^{2+} and Fe^{3+} respectively. But as can be seen from Fig.6 the maximum saturation magnetization is 0.016 μ_B per Fe ion. Furthermore, the values of magnetic moment observed for all the samples are far below than the full moment of Fe^{2+} and Fe^{3+} ions. ZnO crystal structure and charge carrier concentrations. Furthermore, t Thus

the ferromagnetic order of the samples must be due to the exchange interaction between the iron ions and carriers [24]. As can be seen by increasing Fe concentration to 0.07, the distance of the neighboring Fe ions decreases and antiferromagnetic interaction between neighboring Fe–Fe ions suppressed the ferromagnetism at higher Fe doping concentrations

REFERENCES

[1] Ohno H., Toward Functional Spintronics, *Science*, **291**[5505]: 840-841 (2001).

[2] Yang S.Y., Pakhomov A.B., Hund S.T., Wong C.Y., Origin of Room-Temperature Ferromagnetism in Cobalt-Doped ZnO, *IEEE. Trans. Mag*, **38**: 2877-2879 (2002).

[3] Pan F., Song C., Liu X.J., Yang Y.C., Zeng F., Ferromagnetism and Possible Application in Spintronics of Transition-Metal-Doped ZnO Films, *Materials Science and Engineering: R: Reports*, **62**(1), 1-35 (2008).

[4] Özgur Ü., Alivov Y.I., Liu C., Teke A., Reshchikov V., Avrutin, JChoH. Morkoc S., A Comprehensive Review of ZnO Materials and Devices, *J. Appl.Phys.*, **98**(4): 11- (2005).

[5] Pearton S.J., Abernathy C.R., Overberg M.E., Thaler G.T., Norton D.P., Theodoropoulou, N., Hebard A.F., Park Y.D., Ren F.,. Kim J., Boatner L. A.,, Wide Bandgap Ferromagnetic Semiconductors and Oxides, *J. Appl. Phys.*, **93**(1): 1-13 (2003).

[6] Ashok Kumar S., Chen S.M., A Comprehensive Review of ZnO Materials and Devices, *Anal.Lett.*, **41**: 141-158 (2008).

[7] Hung M.H., Mao S., Feick H., Yan H., Wu Y., Kind H., Weber E., Russo R., Yang P., Effects of Local Gas-Flow Field on Synthesis of Oxide Nanowires During, *Science*, **292**: 1897-1899 (2001).

[8] Tirosh E., Markovich G., Control of Defects and Magnetic Properties in colloidal HfO_2 Nanorods, *Advanced Materials*, **19**(18): 2608-2612 (2007).

[9] Wang Q., Sun Q., Chen G., Kawazoe Y., Jena P., Vacancy-Induced Magnetism in ZnO, *Phys. Rev. B*, **77**(20): 205411-   (2008).

[10] Zuo X., Yng S., Yang A., Duan W., Vittoria C., Harris V.G., Ferromagnetism in Pure Wurtzite Zinc Oxide, *J.Appl.Phys.*, **105**(7): 07C508-   (2009).

[11] Zhang S., Ogale S.B., Yu W., Gao X., Liu T., Ghosh S., Das G.P., Wee A.T.S., Greene R.L., Vankatesan T., Comparison of Nb- and Ta-Doping of Anatase TiO_2 for Transparent, *Adv.Mater.*, **21**: 2282-2287 (2009).

[12] Qingyu X., Shengqiang Z., Heidemari S., Magnetic Properties of ZnO Nanopowders, *J. Alloy. Comp.*, **487**: 665-667 (2009).

[13] Kuo C.L., Kou T.J., Huang M.H., Hydrothermal Synthesis of ZnO Microspheres and Hexagonal Microrods with Sheetlike and Platelike Nanostructures, *J. Phys. Chem. B*, **109**: 20115-20121 (2005).

[14] Karthinkeyan B., Pandiyarajan T., Simple room Temperature Synthesis and Optical Studies on Mg Doped ZnO Nanostructures, *J. Lumin.*, **130**: 2317-2321 (2010)

[15] Yadav R.S., Pandey A.C., Sanjay S.S., Optical Properties of Europium Doped Bunches of Zno Nanowires Synthesized by Co-Precipitation Method, *Chalcogenide Let.*, **6**: 233-239 (2009).

[16] Liu C., Meng D., Pang H., Wu X., Xie J., Yu X., Chen L., Liu X., Influence of Fe-Doping on the Structural, Optical and Magnetic Properties of ZnO Nanoparticles, *J. Mag. Mag. Mate.*, **324**: 3356–3360 (2012).

[17] Muneer M.Ba-Abbad Abdul Amir H. Kadhum Abu BakarMohamad Mohd S.Takriff Kamaruzzaman Sopia, Visible Light Photocatalytic Activity of Fe^{3+}-Doped ZnO Nanoparticle Prepared Via Sol–Gel Technique *Chemosphere,* **91**(11): 1604-161 (2013).

[18] Pandiyarajan T., Udayabhaskar R., Karthikeyan B., Role of Fe Doping on Structural and Vibrational Properties of ZnO Nanostructures, *Appl.Phys. A*, **107**: 411-419 (2012).

[19] Kumar S., Gautam S., Kim Y.J., Koo B.H., Chae H., Lee C.G., Ferromagnetism in Fe Doped ZnO Synthesized by Co, *J. Ceram. Soci. Japan*, **1175**: 616-618 (2009).

[20] Kas R., Sevinc E., Topal U., Acar H.Y., A Universal Method for the Preparation of Magnetic and Luminescent Hybrid Nanoparticles, *The Journal of Physical Chemistry C*, **114**(17), 7758-7766 (2010).

[21] Hong Y.Y., Zhang S.Z., Di G.Q., Li H.Z., Zheng Y., Ding J., Wei D.G., Preparation, Characterization and Application of Fe_3O_4/ZnO Core/Shell Magnetic Nanoparticles, *Materials Research Bulletin*, **43**: 2457-2468 (2008).

[22] Bonanni A., Dietl T., A Story of High-Temperature Ferromagnetism in ... - RSC Publishing, *Chem. Soc. Rev.*, **39**: 528-539 (2010).

[23] Yosida K., "Theory of Magnetism", Springer, Berlin, (1996).

[24] Zheng N, Introduction to Dilute Magnetic Semiconductors, Department of Physics and Astronomy, The University of Tennessee, Knoxville (2008).